



Contents lists available at ScienceDirect

# Spectrochimica Acta Part A: Molecular and Biomolecular Spectroscopy

journal homepage: [www.elsevier.com/locate/saa](http://www.elsevier.com/locate/saa)

## Identification of the incommensurate structure transition in biphenyl by Raman scattering

Kai Zhang<sup>a, b, c</sup>, Xiao-Jia Chen<sup>c, \*</sup><sup>a</sup>Key Laboratory of Materials Physics, Institute of Solid State Physics, Chinese Academy of Sciences, Hefei 230031, China<sup>b</sup>University of Science and Technology of China, Hefei 230026, China<sup>c</sup>Center for High Pressure Science and Technology Advanced Research, Shanghai 201203, China

### ARTICLE INFO

#### Article history:

Received 5 June 2018

Received in revised form 30 July 2018

Accepted 31 July 2018

Available online 3 August 2018

#### Keywords:

Biphenyl

Raman spectroscopy

Vibrational properties

Low temperature

### ABSTRACT

Raman scattering measurements are performed on crystalline biphenyl at low temperatures. The properties of the vibrational modes focused on the intra- and intermolecular terms are analyzed in detail. Nearly all of the vibration modes exhibit hardening and simultaneously sharpen with decreasing temperature, whereas the modes at around  $250\text{ cm}^{-1}$  and  $1280\text{ cm}^{-1}$  soften their energies as temperature is decreased. Moreover, all the internal modes have anomalous reversals at around 45 K on the frequencies, widths, and intensities, and below 45 K, several new internal modes appear. Results of the analyses indicate that the reemergence of the interring tilt angle of the molecules at 45 K has a significant impact on the vibrational properties of biphenyl. Our work thus paves interesting and essential groundwork for the further study of biphenyl.

© 2018 Elsevier B.V. All rights reserved.

### 1. Introduction

Poly(*para*-phenylene), as the versatile properties resulted from the delocalized  $\pi$ -electrons, have attracted increasingly intensive interest within the community. These kinds of materials play important roles in the natural explorations of organic materials, and they are already widely applied in real life because of their novel and excellent characteristics compared to inorganic compounds [1–4]. The oligomeric lower members of Poly(*para*-phenylene), which are now named *p*-oligophenyls, always exhibit insulating or semiconducting behaviors in their normal state. However, their conductivity can increase by several orders of magnitude with electron donors or acceptors doping [5–10]. Furthermore, superconducting phases have been discovered in the alkalis-metal doped *p*-oligophenyls [11–17]. It is worth mentioning that the discovery of the superconductivity in *para*-terphenyl with a transition temperature of 123 K [13] is comparable with most cuprate superconductors [18]. On the other hand, the drastic increase of conductivity also makes these materials potentials for thermoelectric applications [19–21]. Poly(*para*-phenylene) materials are composed of phenyl rings connecting in the *para* positions. This typical structure yields two contrary types of forces [22,23], one

is the steric repulsion between the neighboring four H atoms, and the other is the conjugation resulting from the delocalized  $\pi$ -electrons. The competition between these two forces leads to strong thermal librations around the long molecular axis. However, the conformation of the individual molecules at ambient conditions is planar on average as investigated by previous X-ray and neutron diffraction experiments [24–27]. Interestingly, the shake angles of the neighboring rings exhibit stable values arising from the freeze of the molecular librations at low temperature, *i.e.*, the molecules become non-planar [24–27]. The adjacent molecules along the *a* and *b* crystal axes are further confirmed to have the opposite twists. Thus, the lattice parameters along the *a* and *b* directions have double enlargements. Such a transition has been confirmed by specific heat and Raman scattering measurements [28–34]. The nature of this transition in biphenyl is different to other *p*-oligophenyls [35]. The former is “displacive”, whereas the latter is an “order-disorder” type. To make clear the dynamic processes in these materials, it is important to study their structural characteristics and related properties, especially the particular displacive type in biphenyl.

Biphenyl is the shortest oligophenyl with two phenyl rings connected by the single C—C bond. This material is always applied as a starting material for the production of polychlorinated biphenyls or an intermediate for the production of a host of other organic compounds. Previous works [29,30,36–39] showed that biphenyl undergoes two structural transitions at low temperatures. One occurs at 40 K and transforms from phase I of the commensurate monoclinic

☆ Fully documented templates are available in the elarticle package on CTAN.

\* Corresponding author.

E-mail address: [xjchen@hpstar.ac.cn](mailto:xjchen@hpstar.ac.cn) (X.-J. Chen).

system to phase II of the incommensurate triclinic system. The other is phase III that happens at 21 K. The characteristic wave vector of phase II and III are  $q_{\delta} = \delta_a a^* + \frac{1}{2}(1 - \delta_b) b^*$  and  $q_{\delta} = \frac{1}{2}(1 - \delta_b) b^*$ , respectively. Such transitions have also been confirmed by Raman spectroscopy [28,29,40]. Several new peaks appear below 40 K in the low frequency range, and a hard-mode induced by a precursor order appears in the Raman spectra at low temperature [40,41]. So far, even though many works have been performed by Raman spectroscopy, few analyses have focused on the impact that resulted from the transitions on the intrinsic phonon modes located in the high frequency range. Thus, analysis of the properties of those modes are highly desirable to understand the intrinsic physics of biphenyl.

Here, we present the temperature dependent Raman spectra of the pristine biphenyl from 5 K to 300 K excited by a 660 nm laser in the frequency range from the lattice vibrations to the high frequency of the C–H vibrations. The properties of the peaks appearing below 40 K are analyzed in detail by comparing them with previously published data. Furthermore, the anomalies of several modes located at high frequencies are introduced to confirm the structural transition. In the end, a comparison of the physical properties among biphenyl, transition metal dichalcogenides, and cuprate superconductors is performed to understand the physics of the incommensurate structure transition in biphenyl.

## 2. Experimental Details

The biphenyl was purchased from Alfa Aesar. The sample was sealed in a quartz tube with a 1 mm diameter for Raman-scattering experiments in a glove box with the moisture and oxygen levels under than 0.1 ppm. The wavelength of the exciting laser beam was 660 nm. The power was less than 2 mW before a  $\times 20$  objective to avoid possibly damaging the sample. An integration time of 20 s was used to obtain the spectra. The scattered light was focused on the entrance slit of the monochromator which internally contains a 1800 g/mm grating and then recorded with a 1024 pixel Charge Coupled Device designed by Princeton.

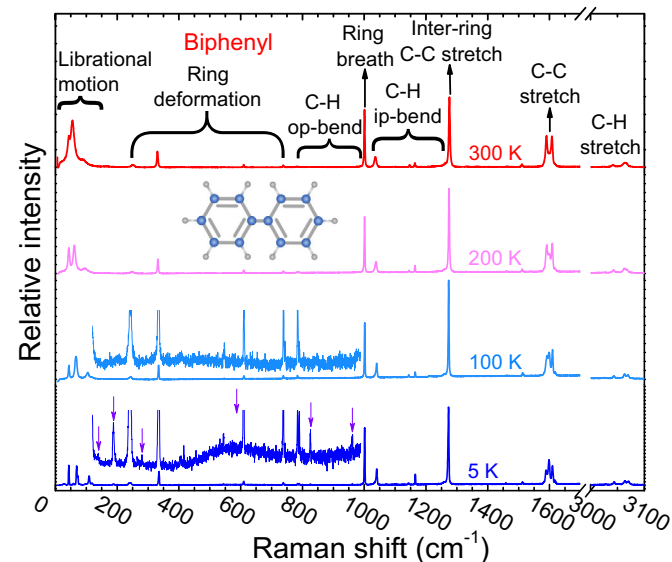


**Fig. 1.** Raman spectra of biphenyl at 300 K, 200 K, 100 K, and 5 K excited by a 660 nm laser, which have been displaced vertically for clarity. The spectra at 5 K and 100 K with the frequencies range of 120–988  $\text{cm}^{-1}$  have been zoomed in for distinguishing the details of the evolution of the spectra with decreasing temperature. Meanwhile, the appeared peaks below 45 K have been pointed out by purple arrows. Classifications of the vibration modes over the spectrum of 300 K were taken from Ref. [42]. Here, op: out-plane, ip: in-plane.

## 3. Results

The 660 nm excited Raman spectra of biphenyl at 300 K, 200 K, 100 K, and 5 K are presented in Fig. 1, and classifications of the vibration modes are depicted over the spectrum at 300 K. All the spectra are placed on the same standard scale. Upon cooling, the spectra of biphenyl are increasingly complex compared to the data recorded at room temperature. Here, the dominating characteristics are summarized:

1. Several phonon modes exhibit obvious splits at low temperature, especially the librational motion modes, the peaks located at around 1600  $\text{cm}^{-1}$ , and the modes with higher frequencies. These splits are also accompanied by the decrease of the full width at half maximum (FWHM) of those peaks. This indicates that the anharmonic effect decreases with decreasing temperature, *i.e.*, the phonon scattering decreases at low temperature.
2. The peak located at around 1000  $\text{cm}^{-1}$ , which is associated with the ring breathing mode, has a little red-shift with decreasing temperature. Meanwhile, as the figure shows, the intensity of this peak has almost no change as temperature changes. Thus, this peak can be used to estimate the trend of the intensities of the other peaks.
3. Below 50 K, a broad weak peak is observed at around 500  $\text{cm}^{-1}$  with the FWHM of above 100  $\text{cm}^{-1}$ . This peak should arise from the formation of the Phase II.
4. Several new internal modes appear at low temperature, such as the peaks located at 137, 188, 280, 824, and 959  $\text{cm}^{-1}$ . The same modes are also observed in the previous works [28,29]. All the modes are vanishingly weak at room temperature.

Details of the phonon modes associated with the librational motion parts are shown in Fig. 2. Biphenyl has a monoclinic system with four planar molecules in one unit cell at ambient conditions [24]. When temperature cools down below 40 K, it undergoes a

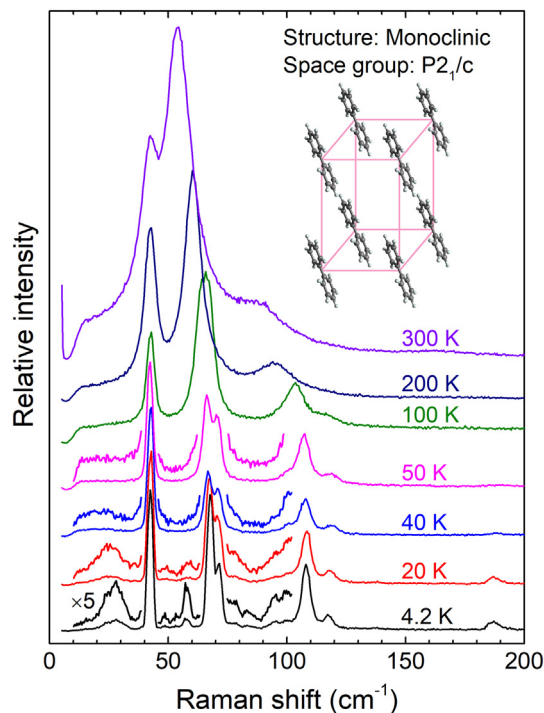


**Fig. 2.** Raman spectra of the librational motions from 0 to 200  $\text{cm}^{-1}$ . The spectra have been displaced vertically for clarity, and several local regions are 5 times amplified. Inset is the crystal structure at room temperature.

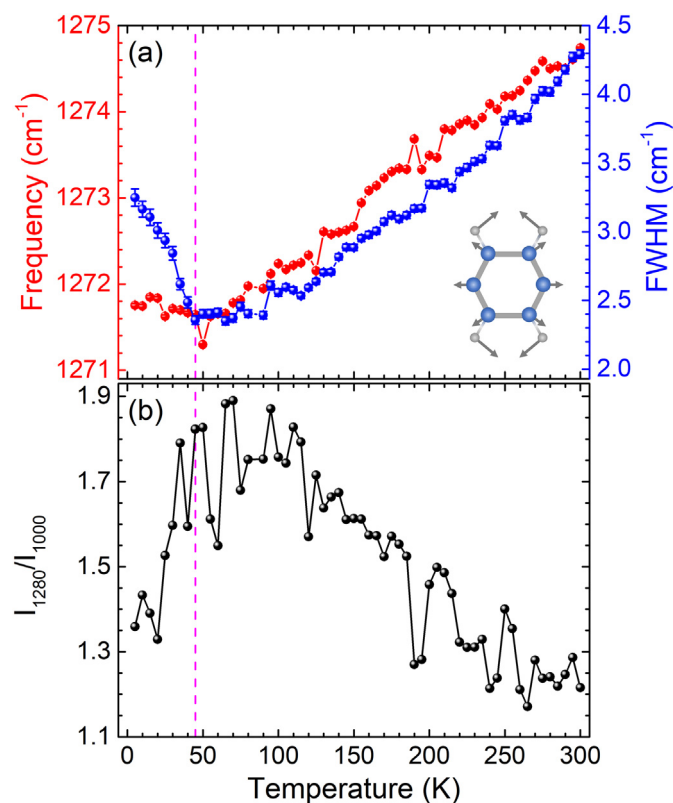


**Fig. 3.** (a) Frequency and FWHM of the  $1280\text{ cm}^{-1}$  mode as a function of temperature. Inset is a schematic diagram of the  $1280\text{ cm}^{-1}$  mode. (b) The ratio of the intensities of the two phonon modes at around  $1280\text{ cm}^{-1}$  and  $1000\text{ cm}^{-1}$ . The vertical dashed lines indicate the structural transition temperature at around  $45\text{ K}$ .

structural transition resulting from the opposite torsional angles of the molecules on the inversion sites [29,37,43]. The angle is confirmed to be about  $10^\circ$  by the neutron diffraction studies [44,45], as well as the low-temperature Raman scattering measurements [29]. Previous works [28,29] reportedly observed several phonon modes below  $40\text{ K}$  by Raman scattering, and interpreted that these modes are associated with the incommensurate phase transition. However,

in our Raman spectra excited by the  $660\text{ nm}$  laser, only one broad peak appears with a frequency of around  $27\text{ cm}^{-1}$ , even though the instrumental resolution is about  $0.5\text{ cm}^{-1}$  (see Fig. 2). This discrepancy should result from the weak Fermi resonant effect due to the low excitation energy. The phonon mode decreases its energy with increasing temperature, and absolutely disappears above  $45\text{ K}$ . This temperature is a little higher than previous works [29]. However, this temperature agrees with the heat capacity measurement [30], which reveals that the thermal anomalies start from  $47\text{ K}$ . Such a behavior indicates that this mode should be the hard-mode [29,40,41]. In addition, several peaks at around  $50, 58, 80,$  and  $100\text{ cm}^{-1}$  also appear below  $50\text{ K}$ , and they share the same behaviors with the hard mode. Thus, those modes also arise from the incommensurate phase transition at around  $40\text{ K}$ . On the other hand, one can see from Fig. 2 that all the phonon modes become sharper with decreasing temperature, even some peaks exhibit splitting at low temperature. Meanwhile, they also increase their energies as temperature is decreased. This indicates that the anharmonic effect decreases with decreasing temperature. This also indicates that the diminishing anharmonic effect is favorable to the structural transition.

The temperature dependent frequency and FWHM of the mode around  $1280\text{ cm}^{-1}$  is depicted in Fig. 3 (a). The ratio of the intensities of this mode and the mode around  $1220\text{ cm}^{-1}$  is always used as an indicator of the conjugation (chain length and planarity) [46–50]. For biphenyl, however, the  $1220\text{ cm}^{-1}$  disappears over the whole temperature range. The  $1280\text{ cm}^{-1}$  is associated with the localized orbitals, which are contributed mainly by the off-axis C atoms, and it is insensitive to the conjugation effects [49]. In our Raman scattering data, an interesting observation is the anomalous behaviors of the frequency and FWHM of this mode. As the figure shows, the frequency and the FWHM all exhibit decreases with the temperature decreases from room temperature to  $45\text{ K}$ . However, below  $45\text{ K}$ , they all increase during cooling. The decreasing FWHM indicates that the anharmonic effect of this mode decreases upon cooling, *i.e.*, the strong thermal librations around the long molecular axis are gradually suppressed with decreasing temperature. Hence, the molecules form quinoid structures. The  $\pi$ -electrons also become more delocalized. This results in the energy of the localized orbitals, *i.e.*, the phonon mode at around  $1280\text{ cm}^{-1}$ , decreasing with decreasing temperature. The reversed increases of the frequency and the FWHM should result from the incommensurate modulation below  $45\text{ K}$  which could create multiple environments in the crystal. The reappearance of the torsion angles will increase the anharmonic effect.

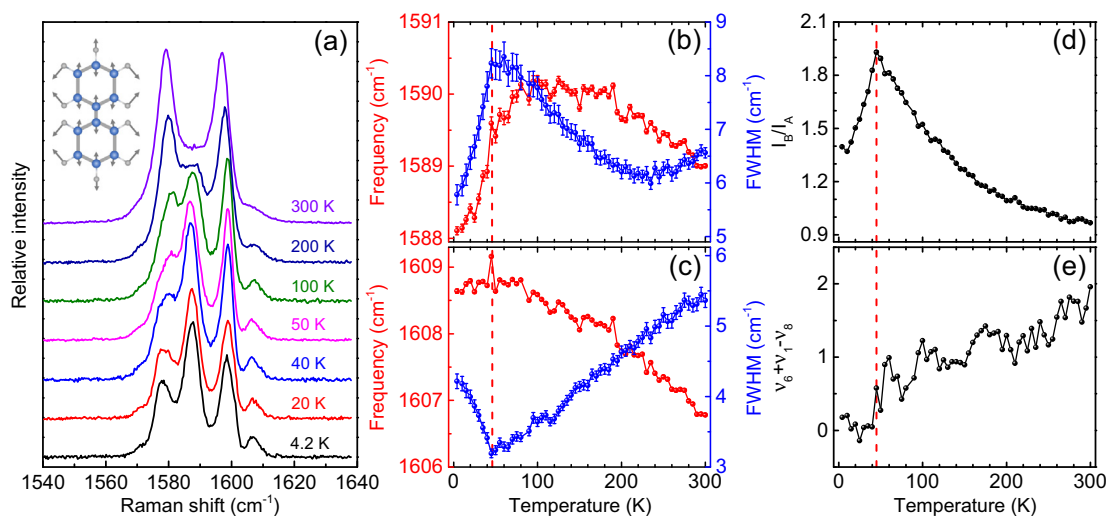


**Fig. 4.** (a) Raman spectra of the modes around  $1600\text{ cm}^{-1}$  of biphenyl. The spectra are displaced vertically for clarity. (b) and (c) are the frequencies and FWHM of the fundamental mode and combination mode around  $1600\text{ cm}^{-1}$ , respectively. (d) Temperature dependence of the  $I_B/I_A$  Ratio. (e) The difference of the  $\nu_6 + \nu_1$  and  $\nu_8$  as a function of temperature. The vertical dashed lines indicate the structural transition temperature at around  $45\text{ K}$ .

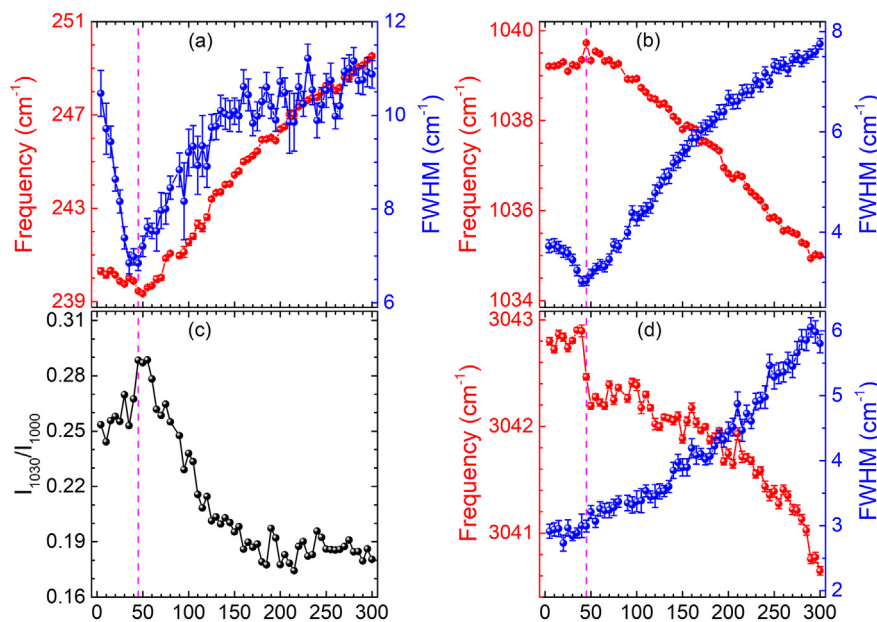


**Fig. 5.** Frequencies of the three phonon modes located at around  $230\text{ cm}^{-1}$  (a),  $1035\text{ cm}^{-1}$  (b), and  $3030\text{ cm}^{-1}$  (d), respectively. (c) Ratio of the intensities of the phonon modes at around  $1030\text{ cm}^{-1}$  and  $1000\text{ cm}^{-1}$ . The vertical dashed lines indicate the structure transition temperature at around  $45\text{ K}$ .

Thus, the frequency and the FWHM all increase below  $45\text{ K}$ . Fig. 3 (b) displays the ratio of the intensities of the  $1280\text{ cm}^{-1}$  mode and the mode around  $1000\text{ cm}^{-1}$ . The ratio increases with decreasing temperature, and then decreases below  $45\text{ K}$ . This tendency corresponds with the temperature dependent tendency of the anharmonic effect.

The mode around  $1600\text{ cm}^{-1}$  also attracts attention due to their interesting properties and is a good indicator of the chain length and planarity [46,50,51]. It always exhibits two strong peaks and one vanishing peak at room temperature. The two strong peaks are suggested to result from the “resonance split”. The peak with the lower energy (A) is a confirmed fundamental band, and the other one with higher energy (B) is related to the combination tone from the  $E_{2g}$  fundamental  $\nu_1$  at around  $992\text{ cm}^{-1}$  and the  $E_{2g}$  fundamental  $\nu_6$  at around  $606\text{ cm}^{-1}$  [51–54]. Upon cooling, these two peaks split to form three sharp peaks. The evolution of the spectra as temperature is increased from  $5\text{ K}$  up to room temperature is shown in Fig. 4 (a). The intensity of the peak A decreases with decreasing temperature, whereas the peak B almost stabilizes its intensity. Meanwhile, a new peak gradually emerges in the middle of the  $1600\text{ cm}^{-1}$  doublet, and simultaneously increases the intensity. The weak peak in the rightmost range increases its intensity upon cooling. We then fitted the doublet by the Lorentz function, and the results are shown in Fig. 4 (b) and (c). The frequencies of these two peaks all increase with decreasing temperature, whereas their FWHM exhibit the opposite tendencies. Moreover, the frequencies and FWHM of these two peaks all have reversed changes below  $45\text{ K}$ . The same anomalies also exist in the other two peaks. This phenomenon indicates that the structural transition also has a significant impact on the modes around  $1600\text{ cm}^{-1}$ .

Fig. 4 (d) is the ratio of the intensities of the two strong peaks A and B at around  $1600\text{ cm}^{-1}$ . One can see that the ratio first monotonously increases with decreasing temperature. Below  $45\text{ K}$ , it exhibits a sharp drop as temperature cools. The ratio is always a good indicator of the conjugation in the case of poly(*para*-phenylene) materials [46,50,51]. It is confirmed that the ratio decreases with decreasing interring tilt angle. However, our experimental data deviates from the situation. Hence, this indicator is not suitable for the low-temperature case. The difference between  $\omega_6 + \omega_1$  and  $\omega_8$  is depicted in Fig. 4 (e). It decreases upon cooling, and becomes stable

to almost 0 below  $45\text{ K}$ . The reduction of the difference indicates that the mixing between the fundamental and combination band declines. Thus, the intensity ratio  $I_B/I_A$  will increase with decreasing temperature [51].

Other phonon modes, such as the modes at around  $230$ ,  $1035$ , and  $3031\text{ cm}^{-1}$ , also exhibit interesting features. The mode at around  $230\text{ cm}^{-1}$  is associated with the ring deformation. The frequency and FWHM of this mode, as seen in Fig. 5 (a), all first decrease with the temperature decreases to  $45\text{ K}$ , and then start to increase with further cooling down. The C–H in-plane bend mode located at around  $1035\text{ cm}^{-1}$  exhibits a different tendency. The frequency of this mode increases upon cooling (seen in Fig. 5 (b)). Below  $45\text{ K}$ , it stops increasing, and even starts to decrease slightly. While the FWHM of this mode has the opposite changes. We also calculate the intensity ratio of the  $1235\text{ cm}^{-1}$  and  $1000\text{ cm}^{-1}$  modes. The result is illustrated in Fig. 5 (c) and shows that the ratio also has a reversal at around  $45\text{ K}$ . The phonon modes at around  $3050\text{ cm}^{-1}$  are associated with the C–H stretch. These modes also exhibit splits at low temperature and increase the intensities. We fitted a strong peak at around  $3040\text{ cm}^{-1}$ , and the results are illustrated in Fig. 5 (d). The frequency of this mode increases with decreasing the temperature. At  $45\text{ K}$ , the energy of this mode has a drastic increase, and then becomes almost constant. The FWHM of this mode decreases over the whole temperature range, whereas the slope of the tendency decreases below  $45\text{ K}$ . All the anomalous features exhibited in these vibration modes indicate that the incommensurate phase transition significantly impacts on the intramolecular vibrational modes.

#### 4. Conclusions

In conclusion, high-quality Raman spectra of the crystalline biphenyl in the temperature range from  $5\text{ K}$  to  $300\text{ K}$  have been performed by laser excitation with a  $660\text{ nm}$  laser. A comprehensive analysis of the vibration modes has been completed to understand the internal properties of biphenyl. The peaks located in the librational motion range all exhibit blue-shift with decreasing the temperature. Below  $45\text{ K}$ , several new internal modes with energies of about  $27$ ,  $50$ ,  $58$ ,  $80$ , and  $100\text{ cm}^{-1}$  appear. The frequency and

FWHM of the inter-ring C—C stretching mode at around 1280 cm<sup>-1</sup> all decrease as temperature decreases, and then increase with further cooling. The intensity of this mode, however, has the opposite change. The energies of the two phonon modes at around 1600 cm<sup>-1</sup> all increase first, and then decrease below 45 K. The ratio of the intensities of these two peaks has the same tendency. Other internal modes are also analyzed in detail. All these phonon modes exhibit anomalies on the frequency, FWHM, and intensity at around 45 K. These results indicate that the reemergence of the interring tilt angle of the molecule at low temperature significantly impacts on the properties of biphenyl. These findings in biphenyl at low temperature are of important significance to understand the physics in biphenyl. Our work paves the way for the further study on biphenyl.

We thank Freyja O'Toole for the language editing.

## Acknowledgments

This work was supported by the National Key R&D Program of China (grant no. 2018YFA0305900).

## References

- N.C. Greenham, S.C. Moratti, D.D.C. Bradley, R.H. Friend, A.B. Holmes, Efficient light-emitting diodes based on polymers with high electron affinities, *Nature* 365 (1993) 628–630.
- C.W. Tang, S.A. VanSlyke, C.H. Chen, Electroluminescence of doped organic thin films, *J. Appl. Phys.* 65 (1989) 3610–3616.
- G. Grem, G. Leditzky, B. Ullrich, G. Leising, Realization of a blue-light-emitting device using poly(*p*-phenylene), *Adv. Mater.* 4 (1992) 36–37.
- G. Grem, G. Leditzky, B. Ullrich, G. Leising, Blue electroluminescent device based on a conjugated polymer, *Synth. Met.* 51 (1992) 383–389.
- E.E. Havinga, L.W. Van Harsen, Dependence of the electrical conductivity of heavily-doped poly-*p*-phenylenes on the chain length, *Synth. Met.* 16 (1986) 55–70.
- D.M. Ivory, G.G. Miller, J.M. Sowa, L.W. Shacklette, R.R. Chance, R.H. Baughman, Highly conducting charge-transfer complexes of poly(*p*-phenylene), *J. Chem. Phys.* 71 (1979) 1506–1507.
- L.W. Shacklette, H. Eckhardt, R.R. Chance, G.G. Miller, D.M. Ivory, R.H. Baughman, Solid-state synthesis of highly conducting polyphenylene from crystalline oligomers, *J. Chem. Phys.* 73 (1980) 4098–4102.
- T. Minakata, M. Ozaki, H. Imai, Conducting thin films of pentacene doped with alkaline metals, *J. Appl. Phys.* 74 (1993) 1079–1082.
- Y. Matsuo, S. Sasaki, S. Ikehata, Stage structure and electrical properties of rubidium-doped pentacene, *Phys. Lett A* 321 (2004) 62–66.
- Y. Kaneko, T. Suzuki, Y. Matsuo, S. Ikehata, Metallic electrical conduction in alkaline metal-doped pentacene, *Synth. Met.* 154 (2005) 177–180.
- R.S. Wang, Y. Gao, Z.B. Huang, X. Chen, Superconductivity in *p*-terphenyl, arXiv:1703.05803.
- R.S. Wang, Y. Gao, Z.B. Huang, X. Chen, Superconductivity at 43k in a single c-c bond linked terphenyl, arXiv:1703.05804.
- R.S. Wang, Y. Gao, Z.B. Huang, X. Chen, Superconductivity above 120 kelvin in a chain link molecule, arXiv:1703.06641.
- J.F. Yan, R.S. Wang, K. Zhang, X. Chen, Observation of Meissner effect in potassium-doped *p*-quaterphenyl, arXiv:1801.08220.
- G. Huang, R.S. Wang, X. Chen, Observation of Meissner effect in potassium-doped *p*-quinquephenyl, arXiv:1801.06324.
- M.V. Mazziotti, A. Valletta, G. Campi, D. Innocenti, A. Perali, A. Bianconi, Possible Fano resonance for high-T<sub>c</sub> multi-gap superconductivity in *p*-Terphenyl doped by K at the Lifshitz transition, *Europhys. Lett.* 118 (2017) 37003.
- G.H. Zhong, X.H. Wang, R.S. Wang, J. Han, C. Zhang, X. Chen, H. Lin, Structural and bonding characteristics of potassium-doped *p*-terphenyl superconductors, *J. Phys. Chem. C* 122 (2018) 3801–3808.
- S.N. Putilin, E.V. Antipov, M. Marezio, Superconductivity above 120k in HgBa<sub>2</sub>CaCu<sub>2</sub>O<sub>6+δ</sub>, *Phys. C* 212 (1993) 266–270.
- N. Dubey, M. Leclerc, Conducting polymers: efficient thermoelectric materials, *J. Polym. Sci.* 49 (2011) 467–475.
- Y. Xuan, X. Liu, S. Desbief, P. Leclère, M. Fahlman, R. Lazzaroni, M. Berggren, J. Cornil, D. Emin, X. Crispin, Thermoelectric properties of conducting polymers: the case of poly(3-hexylthiophene), *Phys. Rev. B* 82 (2010) 115454.
- O. Bubnova, Z.U. Khan, A. Malti, S. Braun, M. Fahlman, M. Berggren, X. Crispin, Optimization of the thermoelectric figure of merit in the conducting polymer poly(3,4-ethylenedioxythiophene), *Nat. Mater.* 10 (2011) 429–433.
- L.A. Carreira, T.G. Towns, Raman spectra and barriers to internal rotation: biphenyl and nitrobenzene, *J. Mol. Struct.* 41 (1977) 1–9.
- J. Soto, V. Hernández, J.T. López Navarrete, Conformational study and lattice dynamics of poly(*p*-phenylene): oligomers and polymer, *Synth. Met.* 51 (1992) 229–238.
- G.P. Charbonneau, Y. Delugeard, Biphenyl: three-dimensional data and new refinement at 293 K, *Acta Cryst.* 33 (1977) 1586–1588.
- P.J.L. Baudour, H. Cailleau, W.B. Yelon, Structural phase transition in polyphenyls. IV. Double-well potential in the disordered phase of *p*-terphenyl from neutron (200 K) and X-ray (room-temperature) diffraction data, *Acta Cryst.* 33 (1977) 1773–1780.
- J.L. Baudour, Y. Delugeard, P. Rivet, Structural phase transition in polyphenyls. VI. Crystal structure of the low-temperature ordered phase of *p*-quaterphenyl at 110 K, *Acta Cryst.* 34 (1978) 625–628.
- Y. Delugeard, J. Desuche, J.L. Baudour, Structural transition in polyphenyls. II. The crystal structure of the high-temperature phase of quaterphenyl, *Acta Cryst.* 32 (1976) 702–705.
- P.S. Friedman, R. Kopelman, P.N. Prasad, Spectroscopic evidence for a continuous change in molecular and crystal structure: deformation of biphenyl in the low temperature solid, *Chem. Phys. Lett.* 24 (1974) 15–17.
- A. Bree, M. Edelson, A study of the second order phase transition in biphenyl at 40 k through Raman spectroscopy, *Chem. Phys. Lett.* 46 (1977) 500–504.
- T. Atake, H. Chihara, Heat capacity anomalies due to successive phase transitions in 1,1-biphenyl, *Solid State Commun.* 35 (1980) 131–134.
- S.S. Chang, Heat capacity and thermodynamic properties of *p*-terphenyl: study of order-disorder transition by automated high-resolution adiabatic calorimetry, *J. Chem. Phys.* 79 (1983) 6229–6236.
- A. Girard, H. Cailleau, Y. Marqueton, C. Ecolivet, Raman scattering study of the order-disorder phase transition in *para*-terphenyl, *Chem. Phys. Lett.* 54 (1978) 479–482.
- K. Saito, T. Atake, H. Chihara, Molar heat capacity and thermodynamic properties of *p*-quaterphenyl, *J. Chem. Thermodyn.* 17 (1985) 539–548.
- K. Saito, Y. Yamamura, M. Sorai, Twist phase transition in poly(*p*-phenylene) oligomers: heat capacity of *p*-quinquephenyl, *Bull. Chem. Soc. Jpn.* 73 (2000) 2713–2718.
- H. Cailleau, A. Girard, F. Moussa, C.M.E. Zeyen, Inelastic neutron scattering study of structural phase transitions in polyphenyls, *Solid State Commun.* 29 (1979) 259–261.
- H. Cailleau, F. Moussa, C.M.E. Zeyen, J. Bouillot, Observation of excitations in the incommensurate phases of biphenyl by inelastic neutron scattering, *Solid State Commun.* 33 (1980) 407–411.
- H. Cailleau, F. Moussa, J. Mons, Incommensurate phases in biphenyl, *Solid State Commun.* 31 (1979) 521–524.
- T. Atake, K. Saito, H. Chihara, Low temperature heat capacities of 1,1'-biphenyl and 1,1'-biphenyl-d<sub>10</sub>, *Chem. Lett.* 12 (1983) 493–496.
- K. Saito, T. Atake, H. Chihara, Incommensurate phase transitions and anomalous lattice heat capacities of biphenyl, *Bull. Chem. Soc. Jpn.* 61 (1988) 679–688.
- M. Wada, A. Sawada, Y. Ishibashi, Soft modes associated with incommensurate phase transitions in biphenyl, *J. Phys. Soc. Jpn.* 50 (1981) 737–738.
- A.D. Bruce, W. Taylor, A.F. Murray, Precursor order and raman scattering near displacive phase transitions, *J. Phys. C* 13 (1980) 483–504.
- K. Honda, Y. Furukawa, Conformational analysis of *p*-terphenyl by vibrational spectroscopy and density functional theory calculations, *J. Mol. Struct.* 735 (2005) 11–19.
- A. Bree, M. Edelson, Further evidence for phase transitions in biphenyl near 40 k and 16 k, *Chem. Phys. Lett.* 55 (1978) 319–322.
- H. Cailleau, J.L. Baudour, C.M.E. Zeyen, Structural phase transition in polyphenyls. VII. A neutron diffraction study of the structural phase transition in biphenyl-d<sub>10</sub>, *Acta Cryst.* 35 (1979) 426–432.
- J.L. Baudour, M. Sanquer, Structural phase transition in polyphenyls. VIII. The modulated structure of phase III of biphenyl (T > 20 K) from neutron diffraction data, *Acta Cryst.* 39 (1983) 75–84.
- H. Ohtsuka, Y. Furukawa, M. Tasumi, Dependencies of the Raman spectra of *p*-oligophenyls on the chain length and the excitation wavelength, *Spectrochim. Acta* 49 (1993) 731–737.
- G. Heimel, D. Somitsch, P. Knoll, E. Zojer, Albrecht theory and anharmonic coupling in polyphenyl raman spectra, *Synth. Met.* 139 (2003) 823–825.
- L. Cuff, M. Kertesz, *Ab initio* oligomer approach to vibrational spectra of polymers: comparison of helical and planar poly(*p*-phenylene), *Macromol.* 27 (1994) 762–770.
- G. Heimel, D. Somitsch, P. Knoll, J.L. Brédas, E. Zojer, Effective conjugation and Raman intensities in oligo(*para*-phenylene)s: a microscopic view from first-principles calculations, *J. Chem. Phys.* 122 (2005) 114511.
- K. Zhang, X.J. Chen, Chain length effects of *p*-oligophenyls with comparison of benzene by Raman scattering, *AIP Adv.* 8 (2018) 025004.
- G. Heimel, D. Somitsch, P. Knoll, E. Zojer, *Ab initio* study of vibrational anharmonic coupling effects in oligo(*para*-phenylenes), *J. Chem. Phys.* 116 (2002) 10921–10931.
- J.E.B. Wilson, Jr, The normal modes and frequencies of vibration of the regular plane hexagon model of the benzene molecule, *Phys. Rev.* 45 (1934) 706–714.
- W.R. Angus, C.R. Bailey, J.B. Hale, C.K. Ingold, A.H. Leckie, C.G. Raisin, J.W. Thompson, C.L. Wilson, Structure of benzene. Part VIII. Assignment of vibration frequencies of benzene and hexadeuterobenzene, *J. Chem. Soc.* 218 (1936) 971–987.
- M. Ito, T. Shigeoka, Raman spectra of benzene and benzene-d<sub>6</sub> crystals, *Spectrochim. Acta* 22 (1966) 1029–1044.